Identification of Obinutuzumab-induced Lysosomal Membrane Permeabilization Modulators via CRISPRi-based Screening in B Cell Lymphoma

Yerim Kim

Department of Medical Science

The Graduate School, Yonsei University

Identification of Obinutuzumab-induced Lysosomal Membrane Permeabilization Modulators via CRISPRi-based Screening in B Cell Lymphoma

Directed by Professor Joo Young Kim

The Master's Thesis
submitted to the Department of Medical Science,
the Graduate School of Yonsei University
in partial fulfillment of the requirements for the degree of
Master of Medical Science

Yerim Kim

December 2023

This certifies that the Master's Thesis of
Yerim Kim is approved.

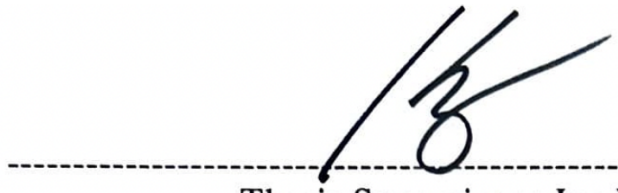

Thesis Supervisor : Joo Young Kim

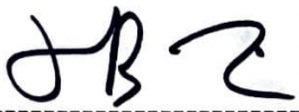

Thesis Committee Member #1 : Hyongbum Kim

Thesis Committee Member #2 : Wan Namkung

The Graduate School
Yonsei University

December 2023

ACKNOWLEDGEMENTS

I would like to extend my heartfelt gratitude to all those who have supported and guided me throughout the journey of completing my Master's thesis.

First and foremost, I owe a tremendous debt of gratitude to my supervisor, Professor Joo Young Kim, for her unwavering support, invaluable guidance, and profound expertise. Your mentorship has been instrumental in shaping this research and my academic growth. Your patience and dedication have been truly inspiring.

I extend my heartfelt thanks to my thesis committee members, Professor Hyongbum Kim and Professor Wan Namkung, for offering insightful advice and profound knowledge.

I would also like to express my sincere appreciation to Dr. Donghyuk Lee, who constantly encouraged me, mentored me, and steered me in the right direction when things were tough. Your dedication to research has been a constant source of motivation, and I am truly thankful for the wisdom you have shared.

I would also like to thank my fellow colleagues, Ayeon, Do Hyeon, Geunah, Beom Jun, Jin Kyung, Hyein, Jihyun and Changsin, who have been my companions in this academic endeavor. Your camaraderie, stimulating discussions, and shared experiences have enriched my research and made this journey much more enjoyable.

Finally, I would like to thank my family members, mom, dad, sister and Happy, for their unwavering support and encouragement throughout my academic pursuits. Your love and belief in me have been my driving force, and I am deeply grateful for everything.

Thank you all.

<TABLE OF CONTENTS>

LIST OF FIGURES

LIST OF TABLES

ABSTRACT

Identification of Obinutuzumab-induced Lysosomal Membrane Permeabilization Modulators via CRISPRi-based Screening in B Cell Lymphoma

Yerim Kim

Department of Medical Science
The Graduate School, Yonsei University

(Directed by Professor Joo Young Kim)

Non-Hodgkin lymphoma (NHL) is a cancer of the lymphatic system that is treated by chemotherapy and CD20-based immunotherapy such as obinutuzumab (OBI). OBI is a second-generation Fc-glycoengineered type II antibody with increased interaction with FcγRIIIa which is expressed on immune effector cells. OBI differs from type I anti-CD20 antibodies in that it promotes greater antibody-dependent cell cytotoxicity (ADCC) and direct cell death (DCD). The major phenotypes of OBI-induced DCD include homotypic adhesion and lysosomal membrane permeabilization (LMP). However, the action mechanism of OBI-induced LMP still remains unclear. Gaining further insight into OBI's mode of action can aid in developing improved therapeutics to treat refractory and relapsed NHL. Here, we used a CRISPRi-based screening approach to identify regulators of OBI-induced LMP and cell death with two goals. The first goal was to identify genes that modulate OBI-induced lysosomal membrane permeabilization using the CRISPRi screening platform, and the second goal was to discover combination therapeutic methods that synergistically enhance OBI-induced DCD. We used a CRISPRi sub-library that targets kinases, phosphatases and drug targets and identified the 15 key negative regulators of OBI-induced LMP. We further validated candidate genes and identified PIKfyve as a key regulator of OBI-induced LMP. We found that PIKfyve inhibition by Apilimod sensitized B cells to OBI-induced LMP. Fission inhibition by Apilimod caused lysosome

coalescence and subsequent vacuolization. Furthermore, Apilimod-induced fission inhibition is in line with TRPML2 inhibition by OBI, which further compounds fission inhibition and increases OBI-induced LMP and DCD. We propose that Apilimod and OBI co-treatment can effectively and synergistically eliminate B cells to treat B cell lymphoma.

Key words: obinutuzumab, B cell lymphoma, non-Hodgkin's lymphoma, anti-CD20 antibodies, lysosomal membrane permeabilization, CRISPR screen, PIKfyve

Identification of Obinutuzumab-induced Lysosomal Membrane Permeabilization Modulators via CRISPRi-based Screening in B Cell Lymphoma

Yerim Kim

Department of Medical Science
The Graduate School, Yonsei University

(Directed by Professor Joo Young Kim)

I. INTRODUCTION

Non-Hodgkin lymphoma (NHL) is a heterogeneous group of hematological malignancies[1]. NHL is derived from B cells, and is clinicopathologically characterized into more than 20 forms, thereby highlighting its diverse nature[2]. The standard care for NHL patients includes chemotherapy and CD20-based immunotherapy such as rituximab and obinutuzumab. In 1997, rituximab was approved by the US FDA to treat relapsed or refractory NHL[3,4]. Rituximab is a type I anti-CD20 antibody and targets malignant B cells for complement-dependent cytotoxicity (CDC), antibody-dependent cellular cytotoxicity (ADCC) and apoptosis [4]. Although rituximab demonstrated early clinical success, a significant portion of patients reported relapse or resistance[2].

Obinutuzumab is FDA-approved for previously untreated follicular lymphoma (FL), relapsed or refractory FL and previously untreated chronic lymphocytic leukemia (CLL)[2]. Obinutuzumab is a second-generation Fc-engineered type II antibody, and was glycoengineered to enhance its interaction with FcγRIIIa expressed on immune effector cells to boost ADCC[5]. An interesting feature of obinutuzumab is that it not

only promotes greater antigen-dependent cell cytotoxicity but also direct cell death (DCD)[6].

In fact, obinutuzumab-induced DCD plays a major role in its cytotoxicity. Herter et al. created an effector-silent Fc variant of obinutuzumab and rituximab by introducing a PGLALA mutation[7]. This effector-silent mutant cannot cause ADCC, ADCP and CDC[7]. When these variants were administered to lymphoma xenograft mouse models, obinutuzumab-PGLALA induced comparable cytotoxicity to rituximab-WT and obinutuzumab-WT treatment caused almost complete tumor regression[7]. This study underscores the significance of obinutuzumab-induced DCD, emphasizing that DCD alone is sufficient for inducing cytotoxicity in lymphoma.

The major phenotypes of obinutuzumab-induced DCD include homotypic adhesion and lysosomal membrane permeabilization (LMP) and membrane damage[8,9]. When cells undergo LMP, the lysosomal content spills into the cytoplasm, resulting in lysosome-dependent cell death[8]. Since cancer cells exhibit altered lysosomal content and activity to meet high energy demands and show weakened lysosomal membranes, targeting the lysosome can be an effective strategy to eliminate malignant tumor cells[8]. Although the exact mechanisms underlying obinutuzumab-induced DCD remain unclear, several studies demonstrate that LMP is necessary for DCD. For example, co-treatment with lysosomotropic reagents such as LLOME and obinutuzumab enhanced DCD in CLL patient-derived cells[10]. Gaining a better understanding of the underlying molecular mechanisms will enable us to improve existing therapies for NHL.

The clustered regularly interspaced short palindromic repeats (CRISPR)-based screening platform is used for large-scale genetic perturbations to probe gene functions[11]. CRISPR interference (CRISPRi) uses a catalytically inactive dead Cas9

(dCas9, mutated RuvC1 and HNH nuclease domains) fused to a KRAB repressor domain[11-13]. The dCas9-KRAB unit is guided by a single guide RNA (sgRNA) to the gene of interest[13]. The sgRNA is designed to target the promoter region, which sterically hinders the interactions between *cis*-acting DNA motifs and *trans*-acting transcription factors[14]. As a result, this system prevents transcription initiation and tunes down gene expression[15].

Lysosomal homeostasis is paramount for maintaining cellular health. Lysosomes are the membrane-bound organelles that house lysosomal enzymes responsible for breaking down and recycling cellular contents[16]. Lysosomal homeostasis is characterized by fusion and fission events[17]. Inhibition of lysosomal fission can have profound implications for cellular stability and response to therapies. Lysosomal fission is a crucial process that regulates the division of lysosomes, maintaining their distribution and function within the cell[18]. When this process is inhibited, lysosomes may coalesce, leading to the formation of larger vacuoles[18]. This disruption in lysosomal dynamics can have detrimental effects on cellular homeostasis, potentially rendering cells more susceptible to destabilization[18]. Understanding the intricate balance of lysosomal dynamics is crucial for developing therapeutic approaches that exploit these processes to benefit medical interventions[18].

In this study, we aimed to elucidate the factors regulating OBI-induced DCD by using the dCas-mediated knock-down system with a sgRNA library targeting kinases, phosphatases and drug targets. The insights gained from this study can serve as the foundation for developing combinatorial therapies aimed at more effectively treating B cell malignancies.

II. MATERIALS AND METHODS

1. Cell culture

Raji B cells (gifted by Prof. Seong Hwan Kim at Chungnam National University) were maintained in Roswell Park Memorial Institute (RPMI)-1640 medium supplemented with 10% fetal bovine serum (FBS) (26140-079) and 1% penicillin-streptomycin (15140-122, Gibco, Life technologies, Carlsbad, CA, USA). Cells were cultured in a humidified incubator (37 °C, 5% CO_2). Raji cells were seeded at a density of 1.0×10^5 cells/ mL and passaged every 2-3 days.

2. Obinutuzumab-WT (OBI-WT) production and purification

10 of 100 mm plates were seeded with 1.0×10^6 cells in complete RPMI and cultured for 1 day at 37°C. On the following day, the culture medium was gently aspirated and replaced with EX-CELL CD CHO media (10743011, Thermofisher) with 1 mM sodium butyrate (LS 033-01, WELGENE, Daegu, Korea). The cells were cultured for 2 weeks at 30 °C. The culture medium containing the secreted antibody was harvested and centrifuged at 1,000 rpm for 3 min and filtered through a 0.45 μM syringe filter to remove cell debris.

The antibody-containing medium was mixed with agarose A beads (Pierce Protein A Agarose, Thermofisher, QE218104) and placed on a rotator overnight at 4°C. The solution was carefully loaded on a gravity filtration column. The beads were washed three times with cold PBS. The antibodies were eluted with 0.1 M citric acid and 1 M Tris. The eluted antibody was loaded onto a dialysis cassette and dialyzed against PBS overnight. The dialyzed antibody was concentrated in an Amicon® Ultra-15 Centrifugal Filter Units (UFC900324, Merck, 3K). The antibody concentration was quantified using NanoDrop™ Lite Spectrophotometer, and the purity was analyzed by SDS-PAGE.

3. Lysosomal membrane permeabilization (LMP) assay

1.0×10^5 Raji cells suspended in 100 μL complete RPMI were treated with 10 μg/mL antibodies (IgG, rituximab, obinutuzumab) for 4 hr at 37°C. Cells were stained with 50 nM Lysotracker Deep Red for 30 min at 37°C prior to sampling. 10,000 events were analyzed by flow cytometry. Cells were gated on whole cells, single cells, and Lysotracker-positive cells.

4. Direct cell death assay

1.0×10^5 Raji cells were resuspended in 100 μL complete RPMI and treated with 10 μg/mL antibodies (IgG, rituximab, obinutuzumab) for 4 hr at 37°C. Cells were stained with 0.25 μM calcein-AM for 30 min at 37°C prior to sampling. 10,000 events were analyzed by flow cytometry. Cells were gated on whole cells, single cells, and calcein-AM-positive cells.

5. CD20 quantification

2.0×10^5 Raji cells were resuspended in 100 μL PBS and treated with 10 μg/mL rituximab for 30 min at 4 °C. Cells were washed once with PBS. Cells were then resuspended with 100 μL PBS treated with 1:500 anti-human Ig Fc-specific FITC-conjugated secondary antibody (109-095-008, 1:200 dilutions; Jackson Laboratories) and incubated for 30 min at 4 °C. Cells were washed once with PBS and resuspended in fresh PBS. 10,000 events were analyzed by flow cytometry for changes in CD20 content.

6. CRISPRi Raji B cell line generation

Raji B cells were lentivirally transduced with SSFV-dCas9-mCherry-KRAB (Addgene #180264). A polyclonal dCas9-Raji B cell line was generated by fluorescence-activated cell sorting (FACS) for mCherry-positive cells. Cells were sorted on the BD FACSAriaIII cell sorter by mCherry fluorescence intensity,

and were divided into mCherry-low, -intermediate, and -high cells. Sorted cells were expanded and validated.

dCas9-Raji B cell lines were validated with sgRNA targeting *MS4A1*, a surface marker for B cells. dCas9-Raji B cell lines were lentivirally transduced with either sgMS4A1 or a non-targeting control (sgERBB2) and treated with 1 μg/mL puromycin (ant-pr-1, Invivogen) to select for knockdown cells. Cells were bound with rituximab, stained with goat anti-human Fc-FITC and analyzed by flow cytometry using LSRII (BD Biosciences) to measure the membrane content of *MS4A1*.

7. sgRNA packaging and transduction

The sgRNA subpooled library targeting kinases, phosphatases and drug targets were a gift from Jonathan Weissman (Addgene #83971). The sgRNA sub-library was first amplified by *E. coli* transformation. Briefly, an aliquot of SS320 electrocompetent *E. coli* was transformed by 50 ng of the sgRNA sub-library by electroporation using the Bio-Rad Gene Pulser II Electroporator using 2.4 kV, 25 μF, and 300Ω. The transformed cells were rescued in 25 mL SOC medium at 37°C, 160 rpm for 30 min. A small aliquot of transformed SS320 cells were serially diluted and plated on agar plates with LB medium and ampicillin to calculate the transformation efficiency. The rest of the transformed cells were cultured overnight in 200 mL LB broth, and the plasmids were extracted by mini-prep.

The sgRNA-sub library was packaged into lentiviral vectors and subsequently delivered to dCas9-Raji cells by lentiviral transduction. Briefly, 10 of 100 mm plates were seeded with 3.0×10^6 HEK293T cells. On the following day when the cells reached 80% confluency, they were transfected with 8 μg sgRNA-sub library, 6 μg psPAX2, 2 μg pMD2.G and 48 μL polyethylenimine (PEI) for 16 hr.

PEI-containing media was gently aspirated and fresh DMEM supplemented with 10% FBS and 1% penicillin-streptomycin was added. After 3 days' post-transfection, the culture supernatant was collected, filtered through a 0.22 μM syringe filter, and the virus was precipitated.

To construct the sgRNA-dCas9-Raji knockdown cell line, 1.3×10^7 dCas9-Raji cells were lentivirally transduced with an initial target transduction rate of 20-50%. The initial transduction efficiency was quantified by flow cytometry for BFP. The knockdown pool was then treated with 0.75 μg/mL puromycin to enrich for stably transduced cells. A stock of cells was prepared by suspending 1.3×10^7 cells with 20% FBS and 10% DMSO in a 2 mL cryovial and storing in a liquid nitrogen tank.

8. CRISPRi screening

1.3×10^7 sgRNA-dCas9-Raji cells (corresponding to 1,000× library coverage) were resuspended in 20 mL complete RPMI and divided in 6-well plates (1.3×10^6 cells/ well). Cells were treated with 10 μg/mL obinutuzumab for 4 hr at 37°C and stained with 50 nM LysoTracker Deep Red for 30 min at 37°C prior to sampling. Cells were harvested, washed once, resuspended in 1 mL complete RPMI and filtered through a Falcon 40 μM cell strainer. Lysotracker-positive cells were sorted using BD FACS Aria III. Recovered cells were cultured in complete RPMI for one week. 1.0×10^5 recovered cells were sampled to measure their lysosomal content by LMP assay. Cells were subject to iterative rounds of FACS until the majority of cells were Lysotracker-positive.

9. CRISPRi genomic DNA (gDNA) isolation

Control cells and obinutuzumab-treated cells were processed for gDNA extraction using Macherey-Nagel's Nucleospin Blood Midi kit following the manufacturer's instructions. Briefly, 1.3×10^7 cells were washed with PBS and

resuspended with 2 ml PBS. Then, the cells were mixed with proteinase K and a lysis buffer and incubated at 56 °C for 15 min. The samples were cooled to room temperature and pure ethanol was added. Then, the lysate was loaded onto a DNA binding column, centrifuged, and washed. Finally, the DNA was eluted using ultrapure DW. The extracted gDNA was loaded on a 1% (w/v) agarose gel and electrophoresed to check the structural integrity.

10. PCR amplification of sgRNA fragments (first round of PCR)

The sgRNA-containing fragments within the gDNA were enriched by PCR. The PCR composition was as follows: 10 μg template, 1 μM forward primer (5'-CAGCACAAAAG GAAACTCACCCTAACTG -3'), 1 μM reverse primer (5'-CGACTCGGTGCCACTTTT -3'), 50 μL NEB Ultra II Q5 2× master mix, DW filled to 100 μL. Roughly 15-20 tubes of 100 μL PCR reactions were set up to amplify the entire gDNA extracts. The sgRNA-containing fragments were amplified using a three-step PCR for 23 cycles in an Applied Biosystems 2720 thermal cycler. The reactions were pooled together, and a small aliquot was loaded on a 1.5% (w/v) agarose gel.

The PCR products (280 bp) were purified using SPRIselect beads (Beckman and Coulter B23317). 300 μL pooled PCR products were used for double SPRI purification. In the first purification round, 300 μL PCR product was mixed with 195 μL SPRI beads (0.65×SPRI beads) and incubated at room temperature for 10 min. In this step, fragments >300 bp bind to the SPRI beads and fragments <300 remain in the supernatant. Then, the tubes were placed on a magnetic stand for 5 minutes to isolate the supernatant with the PCR product. The supernatant was then transferred to new Eppendorf tube for the second round of purification. In this step, 300 μL SPRI beads were added (1×SPRI beads) and thoroughly mixed with the sample. In this step, fragments >150 bp bind to the magnetic beads. After room temperature incubation for 10 min, the tubes were placed back on a

magnetic stand for 5 min. The supernatant was carefully removed, and the beads were washed twice with fresh 80% ethanol. The beads were completely air dried. Finally, the beads were eluted with 20 μL ultrapure DW.

The purified PCR products were run on Agilent 4200 TapeStation using the D1000 kit following the manufacturer's instructions. Briefly, 3 μL sample buffer was added to 1 μL DNA ladder or sample in optical tube strips. The samples were vortexed at 2,000 rpm for 1 min and gently spun down. The tubes were loaded into the instrument and analyzed using TapeStation software.

11. PCR amplification of sgRNA fragments (second round of PCR)

The first PCR products were delivered to Macrogen, a next generation sequencing (NGS) service provider, for the second round of PCR and NGS. Macrogen used the TruSeq Nano DNA (LMW) library kit to ligate the adaptor sequences following the manufacturer's instructions. The index 7 sequences were 5'-TGGCCGGT-3' and 5'-CAATTAAC-3' for the control sample and obinutuzumab-treated sample, respectively. The index 5 sequences were 5'-TAGAGCGC-3' and 5'-CGAGATAT-3' for the control sample and the obinutuzumab-treated sample, respectively. The second PCR products were analyzed using Agilent 4200 TapeStation and the D1000 kit, as described above.

12. Next generation sequencing

The second PCR products were loaded onto a flow cell and placed in the Illumina NovaSeq platform. The PCR products hybridize to the surface-bound oligonucleotides that are complementary to the index 7 and 5 sequences listed above. Then, polymerases, dNTPs and buffers are added to the flow cell for in-situ amplification to promote clustering. Clusters were read by sequencing by synthesis (SBS) chemistry.

13. CRISPRi-sgRNA Screening data analysis

Reads from .fastq files were first trimmed to eliminate the adaptor sequences. Reads were mapped to the kinases, phosphatases, and drug targets sub-pooled library. For both control and obinutuzumab-treated samples, a table of sgRNA read count per guide was generated. Genes were ranked using the Model-based Analysis of Genome-wide CRISPR/Cas9 Knockout (MAGeCK) algorithm[19]. Top screen hits were determined by the robust ranking aggregation (RRA) score, the $\log_2$ fold change (LFC) and the false discovery rate (FDR)[19]. Hit genes with FDR <0.25 were further selected based on DepMap gene perturbation scores, gene expression profiles and inhibitor availability. Figures were generated using GraphPad Prism v9.

14. Validation of CRISPRi hits using construction of individual gene knockdown cell lines

Individual sgRNA targeting hit genes were cloned into the CRISPRi/a V2 library parental plasmid (Addgene #84832). The parental vector was digested with BstXI and BlpI for 2 hr at 37°C and purified by gel extraction. The sense and antisense strands of sgRNA oligonucleotides were synthesized to have BstXI and BlpI overhangs. The pairs of oligos were hybridized by mixing the two strands with 10×T4 Ligation buffer (NEB) and T4 PNK (NEB). The samples were incubated at 37°C for 30 min, then at 95°C for 5 min and finally slowly cooled to 25°C. The annealed oligos were diluted ten-fold. The digested vector, 1 μl diluted oligo duplex, 10× T4 Ligation buffer (NEB) and T4 ligase (NEB) were added to PCR tubes and incubated at room temperature for 2 hr. The ligation products were introduced into DH5α cells using heat shock transformation. Transformed DH5α cells were plated on LB agar plates with ampicillin overnight, and single colonies were inoculated in LB broth the following day and mini-prepped. The extracted plasmids were sequenced using the U6 primer.

dCas9-Raji B cells were lentivirally transduced with the individual gene targeting sgRNA, as described above. Cells were imaged under the fluorescence microscope for BFP two days' post transduction to estimate the transduction efficiency. Cells were treated with 1 μg/mL puromycin two days' post transduction for 1 day and rescued by diluting the viruses with more complete RPMI. The transduction efficiency was quantified by flow cytometry. Individual gene knockdown cell lines were treated with obinutuzumab and Lysotracker Deep Red for LMP assays, as described above.

15. Obinutuzumab-drug combinatorial treatments (cytotoxicity assays)

5.0×10^4 Raji cells were seeded in a 96-well plate and pre-treated with the indicated concentrations of the drugs for 24 hr in a humidified incubator (37°C, 5% CO_2). Then, the cells were treated with the indicated concentrations of obinutuzumab for 4 hr at 37°C, 5% CO_2, and stained with propidium iodide (PI) for 30 min. 10,000 events were analyzed by flow cytometry on BD FACSLyric for changes in the cell morphology as described previously [16]. Briefly, cells were first gated for singlets (based on FSC-A vs. FSC-H scatter), followed by lymphocytes (based on FSC-A and SSC-A scatter). Cell viability was quantified as the percentage of cells in the lymphocytes gate. Cytotoxicity profiles were also analyzed by quantifying PI, a fluorescent dye that binds nucleic acids in dead cells. Cytotoxicity was defined as % PI-positive.

16. Complement-dependent Cytotoxicity (CDC) Assay

5.0×10^4 Raij cells were pre-treated with 50 nM Apilimod for 24 hr in a 96-well plate in a humidified incubator (37°C, 5% CO_2). Cells were treated with increasing concentrations of Rabbit complement-MA and 0.3 μg/mL obinutuzumab-GE and RTX for 1 hr. Cells were stained with PI 30 min prior to flow cytometry. 20,000 events were analyzed by BD FACS. % CDC was defined

as % PI-positive.

17. RNA extraction and quantitative PCR (qPCR)

Raji cells were prepared for RNA extraction using the TRIzol protocol. 3.0×10^6 Raji cells were washed once with PBS and spun down. Cells were resuspended in 500 μl TRIzol and homogenized with vigorous pipetting and vortex. 100 μl chloroform was added, and the two layers were vortexed. Tubes were centrifuged to separate the layers. The aqueous layer was carefully transferred to a new tube and the RNA was washed, dried and eluted in distilled water. The concentration and purity of the RNA samples were checked by nanodrop. cDNA was synthesized using the RNA template, oligo dT primer and reverse transcriptase. qPCR primers were generated by PrimerBank. qPCR was doen following standard protocol for SYBR green.

18. Vacuolization imaging

5.0×10^4 Raji cells were seeded in a 96-well plate and treated with 50 nM Apilimod, 50 μM OSI-027 or 50 μM BAY-1797 for 24 hr. Cells were then stained with 100 nM Lysotracker Red for 30 min. Cells were centrifuged and resuspended in 4 μl RPMI. Cells were mounted on a cover glass visualized under a fluorescent microscope. Vacuoles are shown as red spots.

19. Statistical analysis

Statistical analyses were performed using GraphPad Prism 8 using unpaired student's t test as indicated in the figure legends. Data are presented as mean ± SD. P values are indicated in the figures.

III. RESULTS

1. CRISPR-dCas9 screen uncovers modulators of obinutuzumab-induced LMP

We leveraged the CRISPR-dCas9 screening platform to uncover key modulators of obinutuzumab-induced LMP. A drug-targeting sgRNA sub-library (generously provided by Dr. Weissman) was delivered to dCas9-Raji cells to generate a knockdown pool. Then, cells were subjected to repeated rounds of obinutuzumab and lysotracker treatment and FACS sorting to recover lysotracker-positive cells. We used lysotracker, an intracellular dye that accumulates in acidic organelles, as a marker of LMP and consequently, cell death. After enriching live cells, they were processed for next generation sequencing (NGS) by extracting the genomic DNA (gDNA) amplifying the region of sgRNA diversity. The amplicon was analyzed on an Illumina sequencer and further processed using the MAGeCK algorithm. Depleted and enriched sgRNAs indicated genes that could be targeted with inhibitors and agonists, respectively, to induce synergistic B cell death (Fig 1A).

We first engineered a dCas9-Raji expressing Raji cell line by lentiviral packaging and transduction (Fig 1B). The SSFV-dCas9-mCherry-KRAB vector (generously provided by Dr. Tippale) was transduced into Raji cells and mCherry-expressing cells were sorted on FACSAriaIII. dCas9-expressing Raji cells were validated by transducing them with *MS4A1* (CD20)-targeting sgRNA (Fig 1B). We assessed the knockdown efficiency by quantifying the surface expression of CD20 using flow cytometry (Fig 1E and 1F).

Then, we used the kinase, phosphatase, drug target sgRNA sublibrary (provided by Dr. Weissman) to selectively target known drug targets (Fig 1G). The sub-library targets 2318 genes, with 5 sgRNAs targeting each gene for a total of 12,775 sgRNAs.

To generate the knockdown pool, we first amplified the sgRNA sub-library by electroporation using SS320 electrocompetent *E. coli* cells to ensure 1000× coverage, and then packaged the sub-library into lentiviral vectors. The dCas9-Raji cells were then transduced with these lentiviruses. The initial transduction rate was set between 20% and 50% to ensure that only one sgRNA infected one cell to create single knockdowns and prevent double and triple knockdowns (Fig 1D). Transduced cells were selected with a low dose of puromycin (0.75 μg/mL puromycin), and the selection efficiency was quantified by flow cytometry. 1.3×10^7 cells (to maintain 1000× coverage) were treated with 10 μg/mL obinutuzumab for 4 hr and stained with 50 nM Lysotracker deep red. Lysotracker-positive cells were sorted and enriched. This process was repeated until most cells were unresponsive to obinutuzumab.

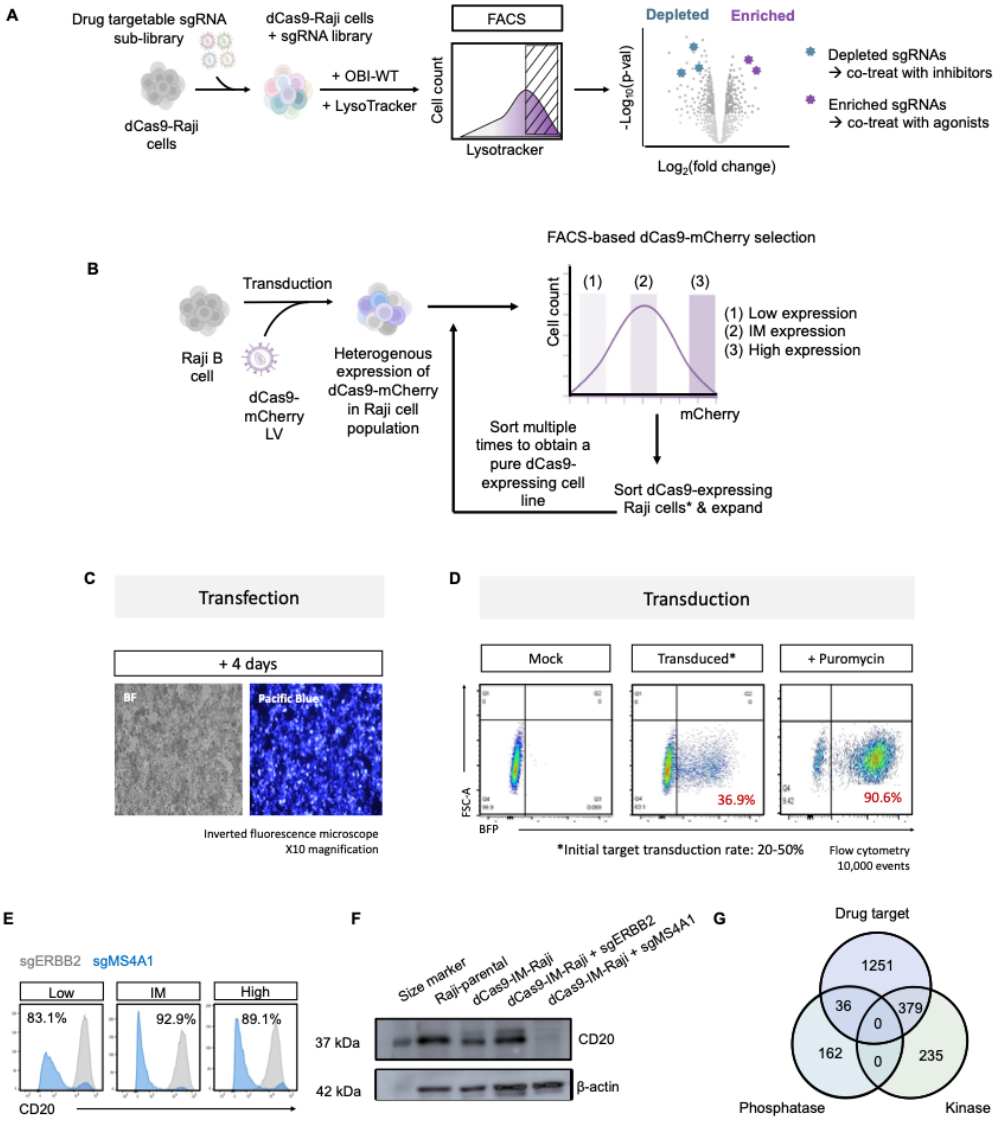

Figure 1. CRISPRi screening workflow to identify modulators of obinutuzumab-induced DCD. **(A)** Schematic of CRISPRi screen. dCas9-Raji cells were lentivirally transduced with a sgRNA sub-library targeting kinases, phosphatases and drug targets (developed by Jonathan Weissman). dCas9-library-Raji cells were treated with 10 μg/ml OBI-WT for 4 hr and stained with 50 nM Lysotracker (LT) for 30 min. LT-positive cells were sorted on FACS Aria III. Cells were expanded, retreated, re-sorted, and processed for NGS analysis. **(B)** Workflow of dCas9-Raji cell line generation. **(C, D)** dCas9-Raji sgRNA knockdown pool generation. **(C)** sgRNA-BFP in transfected HEK293T visualized under a fluorescent microscope. **(D)** Flow cytometry analysis of lentivirally transduced dCas9-Raji cells with sgRNA vector before and after 0.75 μg/mL puromycin selection. **(E, F)** Validation of dCas9-expressing Raji cell lines by **(E)** flow cytometry and **(F)** western blot. **(G)** 2,318 genes from Jonathan Weissman's kinase, phosphatase, drug target CRISPRi sgRNA sublibrary were filtered using Metascape (Uniprot: kinase class, DrugBank: drug targets) and HGNC phosphatase set to identify genes in each functional class.

2. Preliminary experiments showed that iterative FACS-based selection enriches candidate genes

To validate the screening workflow of iterative FACS-based selection, we did a pilot study in which we treated and sorted Raji cells twice. After two rounds of FACS-based selection, we analyzed the cell population by flow cytometry. We found that the sorted cells were still responsive to obinutuzumab (Fig 2A). However, the lysotracker histograms shifted more to the right after the second round of FACS, which indicates that cells were beginning to grow unresponsive (Fig 2A).

Then, we mixed Raji cells with dCas9-sgMS4A1 cells (CD20 knockdown cells) and subjected the pooled cells to two rounds of FACS-based selection. CD20 knockdown cells are unresponsive to obinutzuumab, so if this system works, then we should see an increase in the percentage of CD20 knockdown cells with each round of FACS. Flow cytometry analysis did reveal that each round of FACS enriched the content of CD20 knockdown cells (Fig 2B).

We then moved on to the large-scale experiment, and we treated knockdown pooled cells with obinutuzumab and Lysotracker deep red and subjected them to multiple rounds of FACS to uncover modulators of obinutuzumab-induced LMP and synergistic targets to enhance B cell death. After five rounds of FACS, we analyzed the LMP and DCD rates by flow cytometry (Fig 2C and 2D). Cells grew less responsive to obinutuzumab, and after 5 rounds of FACS, LMP was decreased from 56.1% to 16.0%, and DCD was decreased from 42.6% to 16.8% (Fig 2C and 2D).

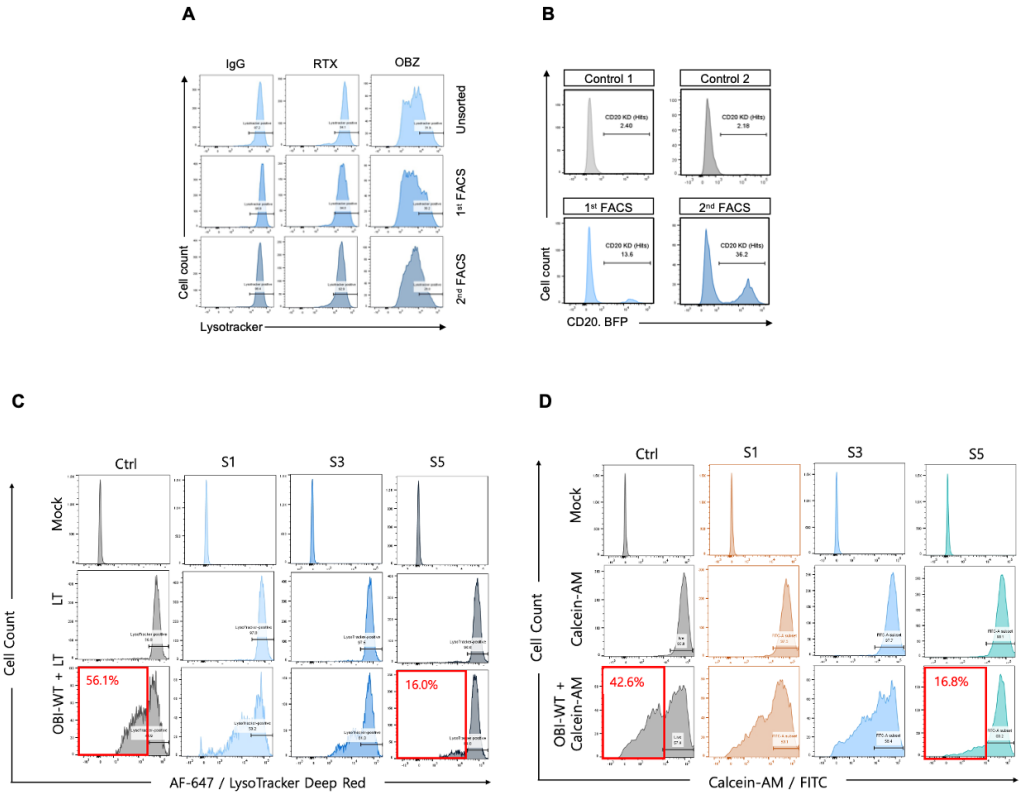

Figure 2. FACS (Cell sorting)-based selection enriches hit genes. (A, B) Preliminary experiments show hit enrichment. **(A)** FACS-sorted lysotracker-positive dCas9-Raji cells were re-treated with OBI-WT and lysotracker. LMP (Lysotracker-negative) rates were analyzed by flow cytometry. Representative histograms are shown. **(B)** The proportion of dCas9-CD20 sgRNA-BFP-Raji cells (positive control) in the total viable sub-population was analyzed. Control cells were passed through the FACS sorter to account for FACS-induced cell damage. Representative histograms are shown. **(C)** LMP Assay with sorted populations for NGS analysis. % LMP (Lysotracker-negative) decreases with successive rounds of cell sorting. **(D)** DCD Assay with sorted populations for NGS analysis. % DCD (calcein-negative) decreases with successive rounds of cell sorting.

3. CRISPRi screen uncovers PIKfyve as a negative regulator of obinutuzumab-induced cell death

CRISPRi screen revealed positive regulators of obinutuzumab-induced cell death. After five rounds of obinutuzumab treatment and FACS-based selection, the enriched cells were prepared for NGS and sequenced on an Illumina sequencer by Macrogen. The reads were processed and further analyzed using the MAGeCK algorithm to rank genes. The volcano plot visualizes the results of the CRISPRi screen (Fig 3A). We found that most genes were depleted in the screen, and this is mostly because known drug targets and kinases are negative regulators of cell death.

We then set up a gene prioritization strategy to filter genes (Fig 3B). First, we selected the FDR cut off at 25%. Second, we used the Cancer Dependency Map (DepMap) database to determine the control sgRNA read count cutoff threshold. Third, we cross-referenced a 2015 Science paper by Wang et al.[20], which details the essential genes in Raji cells. Genes included in this list were excluded. Finally, genes with small molecule inhibitors were selected, and a total of 15 candidate genes were selected for validation. The sgRNA enrichment plots (Fig 3C) and box plots (Fig 3D) show the results of individual genes.

15 candidate genes were further validated using single knockdown cell lines. dCas9-Raji cells were transduced with sgRNA targeting the candidate genes. The knockdown efficiency was quantified by qPCR (Fig 4A). Single knockdown cell lines were subject to LMP and DCD assays (Fig 4B and 4C). Genes showed a good correlation between LMP and DCD (Fig 4D). 6 of the 15 initial candidate genes were selected for further analysis with inhibitor co-treatment. Raji cells were pre-treated with small molecule inhibitors for 24 hr and then were treated with obinutuzumab for 4 hr. We found that co-treatment with small molecule inhibitors and obinutuzumab synergistically killed

Raji cells (Fig 4E and 4F). Of the 6 inhibitors, PIKfyve-targeting Apilimod displayed the most enhanced cell death with obinutuzumab (Figure 4F).

Apilimod and rituximab or obinutuzumab co-treatment induced synergistic direct cell death (Fig 5A). We performed a CDC assay and found that Apilimod treatment does not the influence the CDC activities of both rituximab and obinutuzumab (Fig 5B). We also varied the period of Apilimod exposure, and found that 24 hr pre-treatment, rather than 4 hr treatment of Apilimod induces synergistic cell death (Figure 5B). We reasoned that this difference could be due to vacuolation that is only observed 24-hr post treatment. PIKfyve is a lysosomal lipid kinase that catalyzes the conversion of PIP_2 to $PI(3,5)P_2$[21-23]. PIKfyve is known to regulate lysosomal fission – PIKfyve inhibition by Apilimod blocks lysosomal fission without interfering with fusion, which causes continued lysosomal coalescence and enlargement[23]. We aim to block key regulators of lysosomal fission to gain a better understanding of how Apilimod is able to prime Raji cells for obinutuzumab-induced cell death.

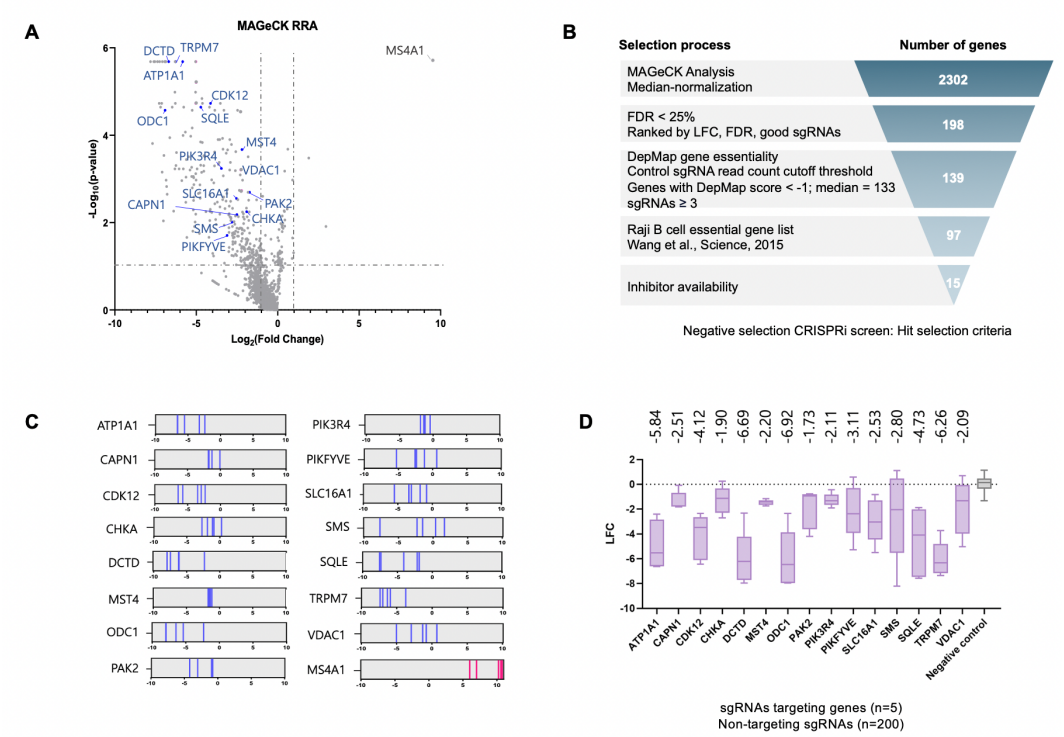

Figure 3. Results of CRISPRi Screening to identify modulators of Obinutuzumab-induced cell death. (A) Volcano plot showing enriched and depleted genes in the screen. Data were analyzed using the Model-based Analysis of Genome-wide CRISPR/Cas9 Knockout (MAGeCK) algorithm. Candidate genes are labelled. **(B)** Hit selection criteria following negative selection. **(C)** sgRNA enrichment plots showing relative positions of 5 sgRNAs/gene. Depleted genes are shown in blue, and a positive control gene (MS4A1, CD20) is shown in pink. **(D)** Box plot showing the LFC per gene. Numbers on top indicate the median LFC for each gene.

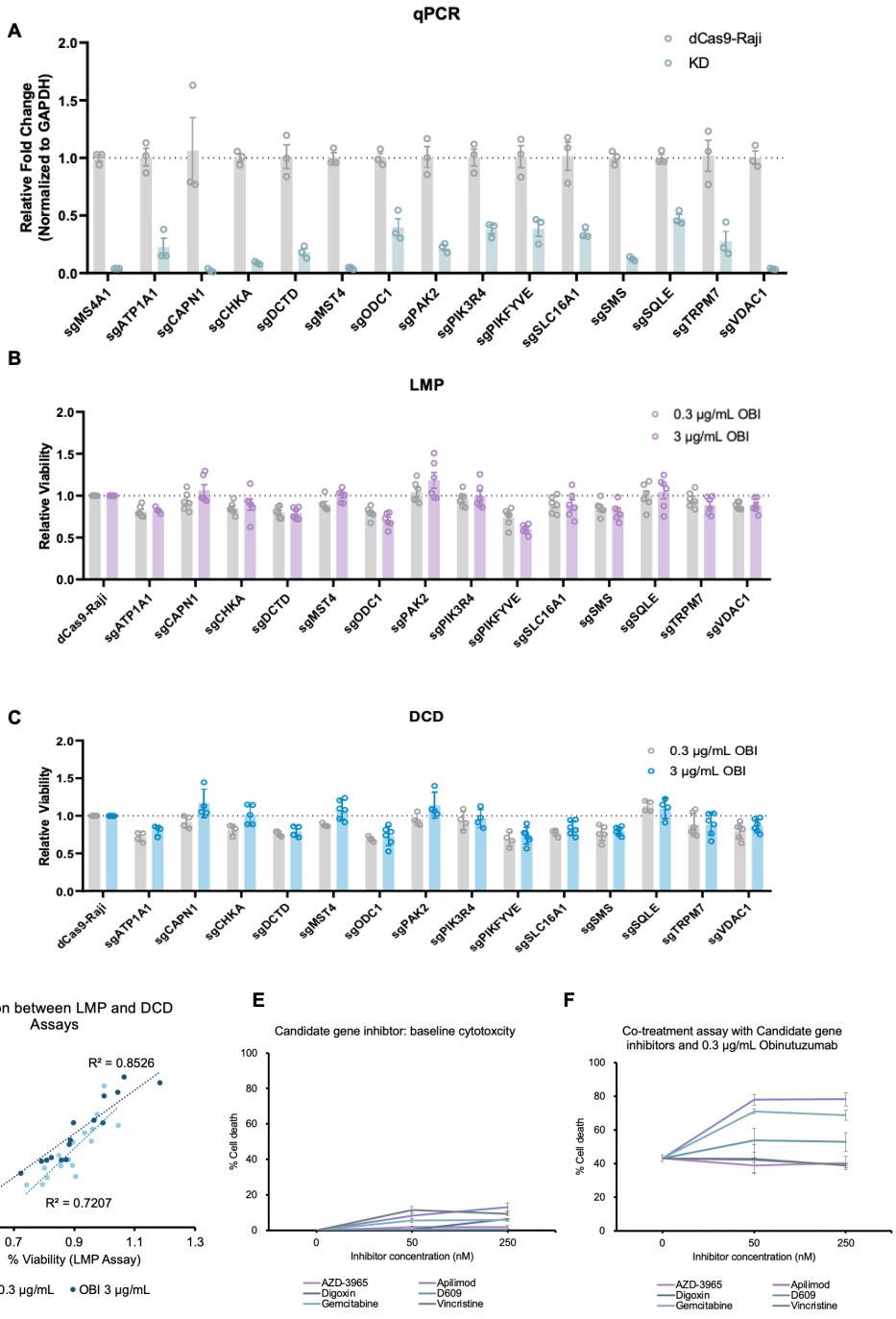

Figure 4. CRISPRi screen identifies PIKfyve as a combinatorial target for obinutuzumab-induced cell death. (A) Knockdown of candidate genes validated by quantitative PCR (qPCR). **(B, C)** LMP and cell morphology-based DCD assays of single knockdown cell lines. **(D)** Correlation between LMP and DCD pathways. **(E, F)** Inhibitor cytotoxicity assay. Cells were pre-treated with the inhibitors for 24 hr and then were treated with 0.3 μg/mL obinutuzumab. Apilimod exhibits superior cytotoxicity compared to other inhibitors at low concentrations. Data are presented as mean ± SD, and the statistical significance was calculated using student's unpaired t test.

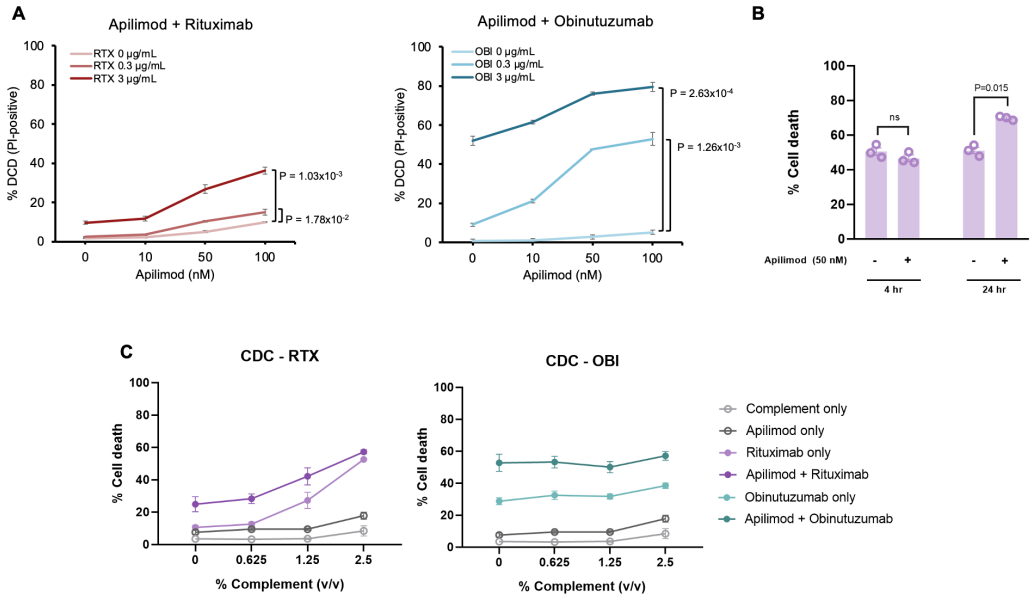

Figure 5. Apilimod and obinutuzumab induce synergistic B cell death. **(A)** Raji DCD assays. Raji cells were pre-treated with Apilimod for 24 hr and then treated with rituximab (left) and obinutuzumab (right) for 4 hr. **(B)** Apilimod and obinutuzumab induce synergistic cell death upon 24 hr pre-treatment. **(C)** Raji CDC assays. Raji cells were pre-treated with Apilimod for 24 hr and then treated with complement and 0.3 μg/mL rituximab or obinutuzumab for 1 hr. Data are presented as mean ± SD, and the statistical significance was calculated using student's unpaired t test.

4. Apilimod and obinutuzumab co-treatment induces superior cytotoxicity by modulating lysosomal fission events

We hypothesized that PIKfyve inhibition by Apilimod and obinutuzumab co-treatment induced superior cytotoxicity due to lysosome vacuolation caused by inhibiting lysosome fission. We investigated other factors that influence lysosomal homeostasis including P2X4 receptor, TRPML2, mTOR and WIPI (Fig 6A). First, we focused on factors involved in lysosome fission, which includes TRPML2, mTOR and WIPI. We expected that co-inhibition of CD20 and these factors listed above would increase cell death, but we only found a significant increase in cell death for MLSI-3 and obinutuzumab co-treatment (Fig 6B-H). Co-inhibition of TRPML2 and CD20 by 10 μM MLSI-3 and 0.3 μg/mL obinutuzumab, respectively, for 4 hr slightly but significantly increased cell death (Fig 6F). TRPML2 is a Ca^{2+} permeable channel that transports Ca^{2+} from the lysosome to the cytoplasm[24-26]. Previous studies using a reporter cell line expressing TRPML2 fused with GCaMP calcium reporter showed that obinutuzumab blocks TRPML2. Obinutuzumab-treated cells did not induce any changes in TRPML2 activity upon the addition of MLSA-1, a TRPML2 agonist. We believe that because obinutuzumab already potently blocks the majority of TPRML2 activity, MLSI-3-induced cell death was only slightly increased. Nevertheless, inhibiting TRPML2 also heightened obinutuzumab-induced cell death, indicating the potential involvement of lysosome fission in enhancing the effects of obinutuzumab-induced cell death.

mTOR plays a role in lysosome fission by phosphorylating dynamin, a motor protein that is involved in membrane scission[27]. We treated cells with OSI-027 to inhibit mTOR and saw vacuolization, which indicated that the drug worked (Fig 6C) [28]. However, we did not find any significant increase in cell death by OSI-027 (Fig 6B).

WIPI2 is a member of the PROPPIN family of proteins[29], regulated by Ca^{2+} released by TRPML2, as well as PIP_2 formed by PIKfyve[29]. WIPI2 interacts with dynamin to control lysosomal fission, and WIPI2 binds to ATG16L1 to induce autophagy[29]. We generated WIPI2 dominant negative mutant cell lines – $WIPI2^{H85E}$ and $WIPI^{R108E}$ to test their involvement in OBI induced DCD[30]. The mutant cell lines and found vacuolization, which indicated that the dominant negative mutation was functioning (Fig 6E). We then treated the mutant cell lines with obinutuzumab, but we unfortunately did not find any significant increase in cell death (Fig 6D).

Finally, P2X4 receptor is a lysosomal membrane protein involved in lysosomal fusion[18]. P2X4 receptor is an ATP-gated Ca^{2+} channel, and it is regulated by lysosomal pH and ATP levels[18]. Once P2X4 receptor gets activated, it releases Ca^{2+} and turns the lysosome basic, which induces lysosome fusion[18]. We treated cells with BAY-1797, a P2X4 receptor inhibitor, and obinutuzumab (Fig 6G). We noted that there was a significant decrease in cell death (Fig 6G). We treated cells with Apilimod and BAY-1797 to test its effects and saw that BAY-1797 treatment rescued Apilimod-induced vacuolization (Fig 6H).

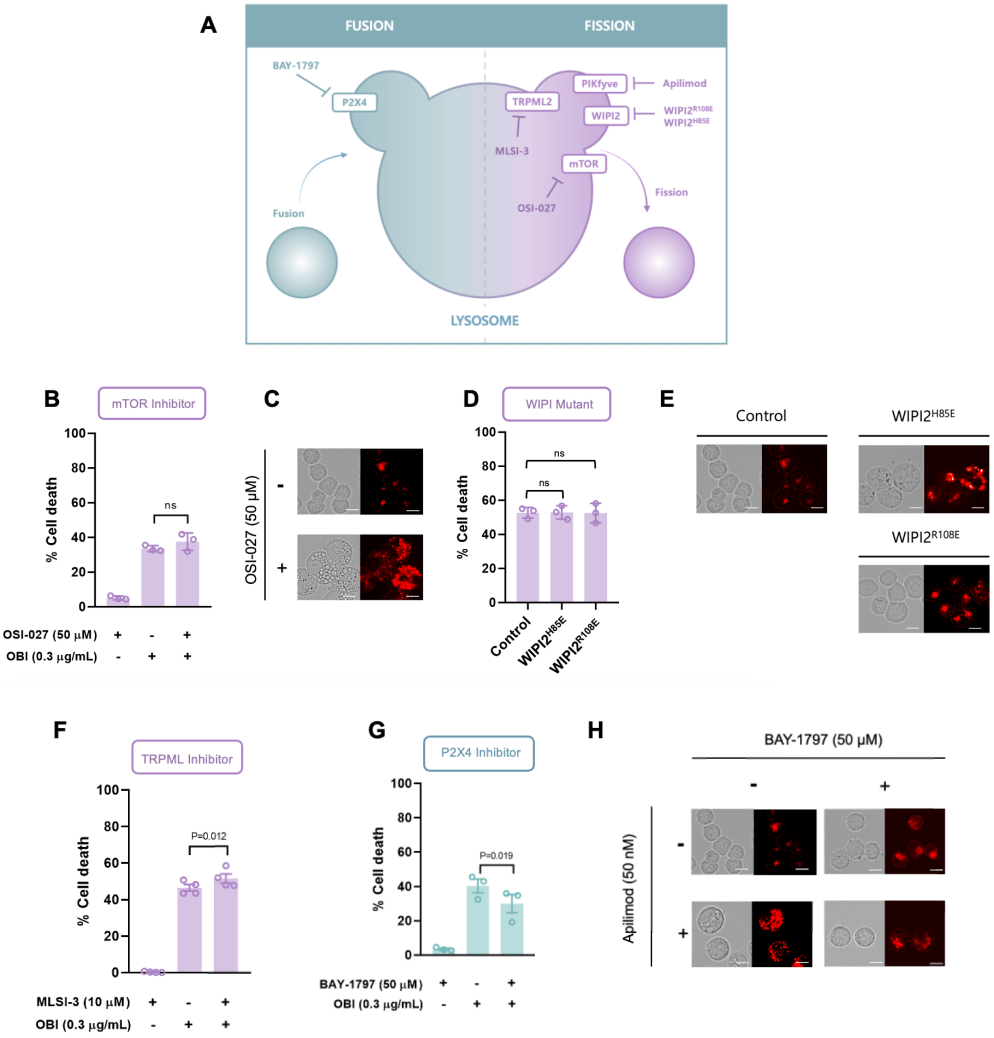

Figure 6. Lysosomal fusion and fission machinery involved in Apilimod and PIKfyve and obinutuzumab activity. **(A)** Diagram of key lysosomal and fission machinery. Fusion inhibition would decrease obinutuzumab-mediated cell, and fission inhibition would increase obinutuzumab-mediated cell death. **(B)** Co-treatment with OSI-027 and obinutuzumab does not induce cell death. **(C)** OSI-027 induces vacuolization. Scale bars indicate 10 μM. **(D)** WIPI2 mutants do not increase obinutuzumab-induced cell death. **(E)** WIPI2 dominant negative overexpression mutants exhibit vacuolization. Scale bars indicate 10 μM. **(F)** Acute co-treatment with 10 μM MLSI-3 and 0.3 μg/mL obinutuzumab

for 4 hr increases cell death. **(G)** Co-treatment with BAY-1797 and obinutuzumab decreases obinutuzumab-induced cell death. **(H)** Apilimod treatment induces vacuolization. BAY-1797 treatment reverses Apilimod-induced vacuolization. Scale bars indicate 10 μM. Data are presented as mean ± SD, and the statistical significance was calculated using student's unpaired t test.

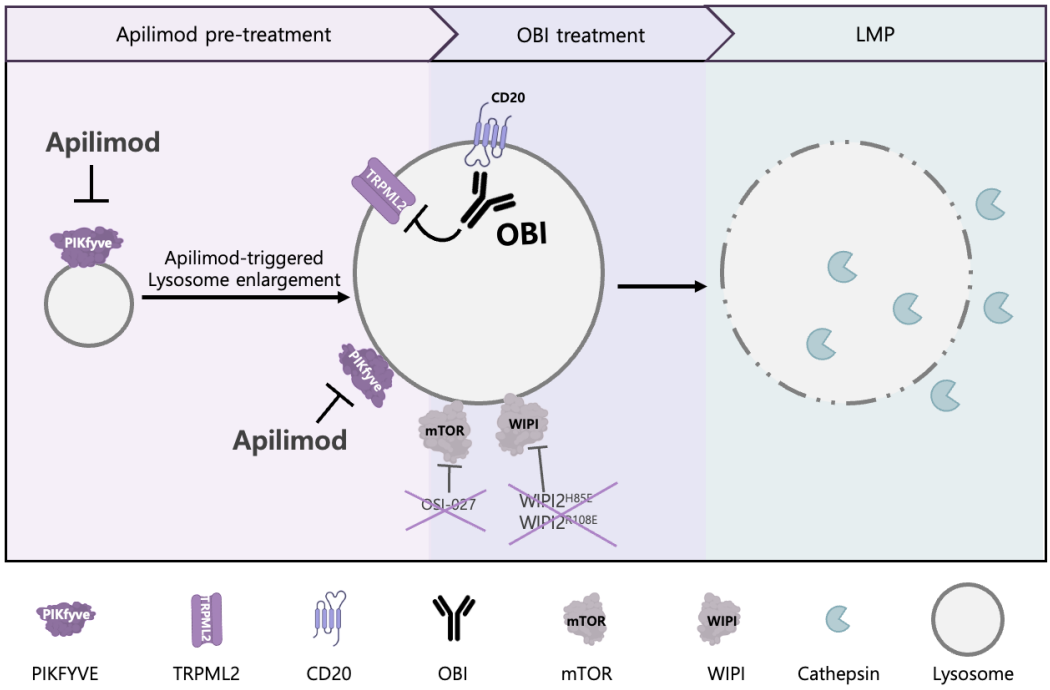

Figure 7. PIKfyve inhibition by Apilimod augments OBI-induced LMP. Schematic illustrating the proposed mechanism for the co-treatment of Apilimod and obinutuzumab. Apilimod pre-treatment induces lysosomal fission inhibition and subsequent lysosome enlargement. Upon obinutuzumab treatment, obinutuzumab endocytoses into the cell and localizes to the lysosome. Obinutuzumab blocks TRPML2 activity, which further inhibits lysosomal fission. Apilimod and obinutuzumab treatment synergistically induces LMP.

IV. DISCUSSION

B cell depletion by anti-CD20 antibodies is an effective treatment strategy for B-NHL[2]. Obinutuzumab, a type II glyco-engineered anti-CD20 antibody elicits DCD and LMP upon antigen recognition and binding[2]. Gaining a better understanding of the inner workings and molecular mechanisms of obinutuzumab can provide grounds to exploit LMP to enhance B cell death. We used the CRISPRi screening platform to identify key modulators of obinutuzumab-induced LMP and DCD, and found PIKfyve, a lysosomal lipid kinase, as a negative regulator of Obinutuzumab-induced cell death.

PIKfyve induces vacuolation and endolysosomal enlargement in B cells and primes them for obinutuzumab-induced cell death[20]. PIKfyve inhibition blocks lysosomal fission while still maintaining fusion, resulting in lysosomal coalescence[21]. This increased lysosomal compartment may sensitize cells to endocytosed obinutuzumab.

Previous studies highlight that obinutuzumab endocytoses into B cells. In the process of endocytosis, obinutuzumab brings neighboring membrane sphingolipids, mainly sphingomyelin, into the lysosome. Sphingomyelin are catabolized by acidic sphingomyelinase, an abundant form of sphingomyelinase in the lysosome, ultimately leading to sphingosine accumulation in the lysosome[31]. Sphingosines are lipids with one hydrophobic lipid tail and act to destabilize the lysosomal membrane[31]. Thus, endocytosed obinutuzumab translocates membrane sphingosines into the lysosome and acts as a trigger for LMP.

Based on the results of this previous study, a potential explanation for Apilimod-based Raji cell sensitization may be that the Apilimod-induced vacuoles are already prone to bursting, and the additional sphingosine brought in by obinutuzumab endocytosis massively triggers LMP and DCD.

In terms of the molecular mechanism underlying this enhanced cytotoxicity, we believe that Apilimod modulates lysosomal fission events, and that the inhibition of these fission events increases obinutuzumab sensitivity. The vacuolization caused by Apilimod is representative of lysosome coalescence due to fission inhibition. To understand the underlying molecular pathways, we identified several factors involved in lysosomal homeostasis including P2X4 receptor that functions in lysosomal fusion and WIPI2, mTOR and TRPML2 involved in lysosomal fission. We hypothesized that lysosomal fusion inhibition would decrease obinutuzumab-induced DCD, and that lysosomal fission inhibition would increase obinutuzumab-induced DCD.

Reducing lysosomal fusion by P2X4 receptor inhibition with BAY-1797 decreased obinutuzumab-induced DCD. We figured that if lysosomal fusion events are inhibited, then this would decrease obinutuzumab endocytosis which would ultimately decrease sphingosine-based lysosome instability and LMP.

On the other hand, reducing lysosomal fission by TRPML2, WIPI2 and mTOR by MLSI-3 treatment, dominant negative mutant formation and OSI-027 treatment, respectively, would theoretically enhance obinutuzumab-induced DCD. Unfortunately, we did not find significant changes in obinutuzumab-induced DCD for WIPI2 and mTOR modulation. However, we did confirm that lysosomal fission inhibition caused by TRPML2 inhibition enhances obinutuzumab-induced DCD. Previous studies also highlight that obinutuzumab blocks TRPML2 activity. A Ramos-GCaMP calcium reporter cell line showed that obinutuzumab blocks TRPML2. Obinutuzumab-treated cells did not induce any changes in TRPML2 activity upon the addition of MLSA-1, a TRPML2 agonist. Here, a further inhibition of TRPML2 by obinutuzumab and MLSI-3 increased obinutuzumab-induced cell death. We believe that genes like PIKfyve and TRPML2 reduce lysosome fission and act to destabilize lysosomes, and ultimately sensitize cells to obinutuzumab-induced LMP and DCD.

V. CONCLUSION

CRISPRi screen identified PIKfyve as a regulator of obinutuzumab-induced LMP and DCD and as a target for combination therapy. Apilimod and obinutuzumab co-treatment presents a novel therapeutic strategy to treat B-NHL.

REFERENCES

1. Shaffer,A., Young, R.M. & Staudt, L.M. Pathogenesis of Human B Cell Lymphomas. Annual Reviews Immunology, 30, 565-610 (2012).
2. Plosker, G.L., & Figgit, D.P. Rituximab. A Review of its Use in Non-Hodgkin's Lymphoma and Chronic Lymphocytic Leukemia. Drugs, 63, 803-843 (2003).
3. Banerjee, T. & Vallurupalli, A. Emerging New Therapies/Immune Therapies in B Cell Non-Hodgkin's Lymphoma. Current Problems in Cancer, 46, 1 (2022).
4. Pierpont, T.M., Limper, C. B. & Richards, K.L. Past, Present, and Future of Rituximab – The World's First Oncology Monoclonal Antibody Therapy. Frontiers in Oncology, 8 (2018).
5. Umana, P., Ekkehard, M., Peter, B., Gabriele, K., Ursula, P., Suter, T. et al. GA101, a Novel Humanized Type II CD20 Antibody with Glycoengineered Fc and Enhanced Cell Death Induction, Exhibits Superior Anti-Tumor Efficacy and Superior Tissue B Cell Depletion In Vivo. Blood, 110, 11, 2348 (2007).
6. Honeychurch, J., Alduaji, W., Azizyan, M., Cheadle, E.J., Pelicano, H., Ivanov, A. et al. Antibody-induced nonapoptotic cell death in human lymphoma and leukemia cells is mediated through a novel reactive oxygen species-dependent pathway. Blood, 119 (15), 3523-3533 (2012).
7. Herter, S., Herting, F., Muth, G., van Puijenbroeck, E., Schlothauer, T., Ferrara, C. et al. GA101 P329GLALA, a variant of obinutuzumab with abolished ADCC, ADCP and CDC function but retained cell death induction, is as efficient as rituximab in B-cell depletion and antitumor activity. Haematologica, 103(2) (2018).
8. Alduaji, W., Ivanov, A., Honeychurch, J., Cheadle, E.J., Potluri, S., Lim, S.H. et al. Novel Type II anti-CD20 Monoclonal Antibody (GA101) Evokes Homotypic Adhesion and Actin-dependent, Lysosome-mediated Cell Death in B-cell Malignancies, Blood, 117 (17), 4519-29 (2011).
9. Kim, J.R., Lee, D., Kim, Y., Kim, J.Y. CD20/TNFR1 dual-targeting antibody

enhances lysosome rupture-mediated cell death in B cell lymphoma, Cancer Immunology, Immunotherapy, 72, 1567-1580 (2023).

10. Constantinides, M., De Maudave, A.F., Potier-Cartereau, M., Campos-Mora, M., Cartron, G., Villalba, M. Direct Cell Death Induced by CD20 Monoclonal Antibodies on B Cell Lymphoma Cells Revealed by New Protocols of Analysis. Cancers, 15 (4), 1109 (2023).
11. Qi, L.S., Larson, M.H., Gilbert, L.A., Doudna, J.A., Weissman, J.S., Arkin, A.P. et al. Repurposing CRISPR as an RNA-Guided Platform for Sequence-Specific Control of Gene Expression. Cell, 152 (5), 1173-1183 (2013).
12. Larson, M.H., Gilbert, L.A., Wang, X., Lim, W.A., Weissman, J.S., Qi, L.S. CRISPR Interference (CRISPRi) for Sequence-specific Control of Gene Expression. Nature Protocols, 8, 2180-2196 (2013).
13. Gilbert, L.A., Horlbeck, M.A., Adamson, B., Villalta, J.E., Chen, Y., Whitehead, E.H. et al. Genome-scale CRISPR-Mediated Control of Gene Repression and Activation. Cell, 159, 3, 647-661 (2014).
14. Horlbeck, M.A., Gilbert, L.A., Villalta, J.E., Adamson, B., Pak, R.A., Chen, Y. et al. Compact and Highly Active Next-Generation Libraries for CRISPR-mediated Gene Repression and Activation. Elife, 5 (2016).
15. Kampmann, M., Horlbeck, M.A., Chen, Y., Tsai, J.C., Bassik, M.C., Gilbert, L.A. et al. Next-generation Libraries for Robust RNA Interference-based Genome Wide Screens. PNAS, 112, 3384-3391 (2015).
16. Iulianna,T., Kuldeep, N., Eric, F. The Achilles' Heel of Cancer: Targeting Tumors via Lysosome-induced Immunogenic Cell Death. Cell Death & Disease, 13, 509 (2022).
17. Wang, F., Gomez-Sintes, R., Boya, P. Lysosomal membrane permeabilization and cell death. Traffic, 19, 918-931 (2018).
18. Saffi, G.T. & Botelho, R.J. Lysosome Fission: Planning for an Exit. Trends in Cell Biology, 29(8), 635-646 (2019).
19. Li, W., Xu, H., Xiao, T., Cong, L., Love, M.I., Zhang, F. et al. MAGeCK Enables

Robust Identification of Essential Genes from Genome-scale CRISPR/Cas9 Knockout Screens. Genome Biology, 15, 554 (2014).

20. Wang, T., Birsoy, K., Hughes, N.W., Krupczak, K.M., Post, Y., Wei, J.J. et al. Identification and characterization of essential genes in the human genome. Science, 350(6264), 1096-1101 (2015).
21. Min, S.H., Suzuki, A., Guzman, J. & Abrams, C.S. Pikfyve Is Essential for Lysosomal Homeostasis in Macrophages. Blood, 124(21), 461 (2014).
22. Gayle, S., Landrette, S., Beeharry, N., Conrad, C., Hernandez, M., Beckett, P. et al. Identification of apilimod as a first-in-class PIKfyve kinase inhibitor for treatment of B-cell non-Hodgkin lymphoma. Blood, 128(13), 1768-1778 (2017).
23. Bissig, C., Hurbain, I., Raposo, G. & van Niel, G. PIKfyve activity regulates reformation of terminal storage lysosomes from endolysosomes. Traffic, 18(11), 747-757 (2017).
24. Immanuel, T., Li, J., Green, T.N., Bogdanova, A. & Kalev-Zylinska, M.L. Deregulated calcium signaling in blood cancer: Underlying mechanisms and therapeutic potential. Frontiers in Oncology, 12 (2022).
25. Heo, W., Jin, N., Park, M.S., Kim, H.Y., Yoon, S.M., Lee, J. et al. Stim1 knock-down decreases the affinity of obinutuzumab for Cd20 by altering Cd20 localization to triton-soluble membrane. Clinical and Experimental Immunology, 200(3), 260-271 (2020).
26. Chen, C., Krogsaeter, E., Butz, E.S., Li, Y., Puertollano, R., Wahl-Schott, C. et al. TRPML2 is an osmo/mechanosensitive cation channel in endolysosomal organelles. Science Advances, 6(46) (2020).
27. Puertollano, R. mTOR and lysosome regulation. F1000Prime Rep, 6(52) (2014).
28. Srivastava, R.K., Li, C., Khan, J., Banerjee, N.S., Chow, L.T. & Athar, M. Combined mTORC1/mTORC2 inhibition blocks growth. Proceedings of the National Academy of Sciences, 116(49), 24583-24592 (2019).
29. Shimizu, T., Tamura, N., Nishimura, T., Saito, C., Yamamoto, H. & Mizushima, N.

Comprehensive analysis of autophagic functions of WIPI family proteins and their implications for the pathogenesis of β-propeller associated neurodegeneration. Human Molecular Genetics, 32(16), 2623-2637 (2023).

30. Strong, L.M., Chang, C., Riley, J.F., Boecker, C.A., Flower, T.G., Buffalo, C.Z. et al. Structural basis for membrane recruitment of ATG16L1 by WIPI2 in autophagy. eLife, 10 (2021).
31. Gorelik, A., Illes, K., Heinz, L.X., Superti-Furga, G. & Nagar, B. Crystal structure of mammalian acid sphingomyelinase. Nature Communications, 7 (2016).

APPENDICES

Table 1. Information of kinase, phosphatase and drug target sgRNA sublibrary, designed by Jonathan Weissman, MIT

Sublibrary	Genes	5 sgRNAs/gene
Kinases, Phosphatases, Drug Targets	2318	130,025
Cancer and Apoptosis	2916	16,325
Stress and Proteostasis	3093	16,905
Mitochondria, Trafficking, Motility	2219	12,300
Gene Expression	2292	12,715
Membrane Proteins	2418	13,205
Unassigned	3649	20,060
Genome-scale	18,905	104,535

Table 2. CRISPRi screen results analyzed by MAGeCK algorithm

Label	Reads	Mapped	Mapped %	TotalsgRNAs	Zerocounts	GiniIndex
Control.fastq	11095601	4856811	43.8	13008	33	0.0695
Sample.fastq	7908527	3457636	43.7	13008	463	0.1596

Table 3. List of sgRNA oligonucleotide sequences

Gene	Direction	Sequence
ATP1A1	F	TTG GGAGGGAGCGCAGTAACGGG G TTT AAG AGC
	R	TTA GCT CTT AAAC CCCGTTACTGCGCTCCCTCC CAA CAA G
CAPN1	F	TTG GCACCGGGAAGCCAGCCTCA G TTT AAG AGC
	R	TTA GCT CTT AAAC TGAGGCTGGCTTCCCGGTGC CAA CAA G
CHKA	F	TTG GCGGGCGGCCGCAGCGCGAG G TTT AAG AGC
	R	TTA GCT CTT AAAC CTCGCGCTGCGGCCGCCCGC CAA CAA G
DCTD	F	TTG GGCGCGGAGCCGGCACCGGA G TTT AAG AGC
	R	TTA GCT CTT AAAC TCCGGTGCCGGCTCCGCGCC CAA CAA G
MST4	F	TTG GAGGGCCGCCGAACTACCCC G TTT AAG AGC
	R	TTA GCT CTT AAAC GGGGTAGTTCGGCGGCCCTC CAA CAA G
ODC1	F	TTG GTAGGGAGCGGCGTGCCGTG G TTT AAG AGC
	R	TTA GCT CTT AAAC CACGGCACGCCGCTCCCTAC CAA CAA G
PAK2	F	TTG GCGGAGTCCTGCGCACGCCA G TTT AAG AGC
	R	TTA GCT CTT AAAC TGGCGTGCGCAGGACTCCGC CAA CAA G
PIK3R4	F	TTG GCC AGC AGC TGG AGC GGA GT G TTT AAG AGC
	R	TTA GCT CTT AAA CAC TCC GCT CCA GCT GCT GGC CAA CAA G
PIKFYVE	F	TTG GAGTCGGCCCCCGAGAGCGG G TTT AAG AGC
	R	TTA GCT CTT AAAC CCGCTCTCGGGGGCCGACTC CAA CAA G
SLC16A1	F	TTG GTGGCTAGCTGCGTGGGTAC G TTT AAG AGC
	R	TTA GCT CTT AAAC GTACCCACGCAGCTAGCCAC CAA CAA G
SMS	F	TTG GCTGGGAGTGTGCTGCGCCC G TTT AAG AGC
	R	TTA GCT CTT AAAC GGGCGCAGCACACTCCCAGC CAA CAA G
SQLE	F	TTG GCACCAGCATCCCTCGCGGG G TTT AAG AGC
	R	TTA GCT CTT AAAC CCCGCGAGGGATGCTGGTGC CAA CAA G
TRPM7	F	TTG GCGGCCTGTAGCCATCTATC G TTT AAG AGC
	R	TTA GCT CTT AAAC GATAGATGGCTACAGGCCGC CAA CAA G
VDAC1	F	TTG GCCCGCCGCCACATCCTCTG G TTT AAG AGC
	R	TTA GCT CTT AAAC CAGAGGATGTGGCGGCGGGC CAA CAA G

Table 4. List of qPCR primer sequences designed by PrimerBank

Gene	Primer sequences		Tm (°C)	Amplicon size (bp)	PrimerBank ID
ATP1A1	F	ACAGACTTGAGCCGGGGATTA	62.7	100	237681108c1
	R	TCCATTCAGGAGTAGTGGGAG	60		
CAPN1	F	GCCAAGCAGGTGAACTACC	60.4	125	311893361c3
	R	TATGGGTCCACGTTGTTCCAC	62		
CHKA	F	ATTACAGGGGATTCGACATTGGA	61.1	117	47078275c3
	R	GCTGTTGTTTCTTGGTGGGAT	60.8		
DCTD	F	CCAAATGGGTGCAGTGATGAC	61.5	138	61742818c2
	R	ACTACAGCCTTTCACATCGGT	61.1		
MST4	F	ATCTTGTGCAAACCCTGAGTTG	61	104	109633024c2
	R	TTCAATCGCCTGATTCCTGCT	61.8		
ODC1	F	TTTACTGCCAAGGACATTCTGG	60.2	127	4505488c1
	R	GGAGAGCTTTTAACCACCTCAG	60.3		
PAK2	F	CACCCGCAGTAGTGACAGAG	61.9	112	191250770c3
	R	GGGTCAATTACAGACCGTGTG	60.6		
PIK3R4	F	GCTCTTTAGGCAGTATGTGCG	61.1	148	116812580c3
	R	GATGTCCCCATGACGAACTCC	62.2		
PIKFYVE	F	ACCTCCGAGCTTGCACATATT	61.5	95	295789161c2
	R	TGAAAGAGCATTCAAGTCTTCCC	60.5		
SLC16A1	F	GGTGGAGGTCCTATCAGCAGT	62.7	107	115583684c2
	R	CAGAAAGAAGCTGCAATCAAGC	60.4		
SMS	F	TGGGCGGGTGAAACGATTAC	62.5	162	311083638c1
	R	CCAAACTGCTTCGAGTGTAGAA	60.2		
SQLE	F	GATGATGCAGCTATTTTCGAGGC	60.7	179	62865634c2
	R	CCTGAGCAAGGATATTCACGACA	60		
TRPM7	F	GTTGGAAAGTATGGGGCGGAA	62.4	190	296080776c2
	R	CACACACAACTACTGGAACAGG	60.8		
VDAC1	F	CTGACCTTCGATTCATCCTTCTC	62.4	75	307133764c1
	R	CTCCCGCTTGTACCCTGTC	63		

ABSTRACT (IN KOREAN)

B세포 림프종에서 CRISPRi 스크린을 이용한 오비누투주맙 유도 라이소좀 붕괴 조절인자 발굴

<지도교수 김주영>

연세대학교 대학원 의과학과

김예림

비호지킨 림프종(NHL)은 림프계통의 암으로, 화학 요법 및 obinutuzumab (OBI)와 같은 CD20 기반 면역요법으로 치료됩니다. OBI 는 FcɣRⅢa 를 발현하는 면역 효능 세포와의 상호 작용을 증가시킨 2 세대 Fc 변형기술이 적용된 2 형 항 CD20 항체로, 높은 항체 의존 면역세포 매개 세포독성 뿐 아니라 결합 만에 의한 직접적인 세포 사멸 (DCD)을 촉진하는 특징을 갖습니다. OBI 로 유발된 DCD 의 주요 형질은 리소좀 막 투과성 (LMP)을 반드시 거치는 것으로 알려져 있지만 그러나 OBI 로 인한 LMP 의 정확한 작용 메커니즘은 아직 불분명합니다. 본 연구는 OBI 로 유발된 LMP 와 DCD 에 대해 이해하고, OBI 기반 DCD 를 향상시키기 위한 새로운 병용약물 및 병용치료의 분자 메커니즘 제안을 목표로 합니다. 본 연구에서는 OBI 로 유발된 LMP 의 조절인자를 발굴하기 위해 CRISPRi 기반의 스크리닝 접근법을 사용하였습니다.

PIKfyve의 발현감소는 OBI로 유발된 LMP와 DCD를 유의하게 감소시켰으며, 그 억제제인 Apilimod 처리는 라이소좀 분열 (fission)을 억제하고, 세포 내 소포체증가 (vacuolization)를 유도하여 OBI에 대한 민감도를 증진하였습니다. mTOR, WIPI 등의 라이소좀 분열과 관련된 다른 기전이 아닌, PIKfvye의 억제가 OBI에 의한 TRPML2의 기능 억제와 동반되었을 때 LMP와 DCD가 증가되었습니다. 본 연구가 제안한 OBI에 의한 LMP조절 기전의 규명은 Apilimod 와 OBI 병용치료법을 B 세포 림프종의 새로운 치료방법으로 제안하는 기반 지식을 제공합니다.

핵심되는 말 : B 세포 림프종, 오비누투주맙, 크리스퍼 스크리닝, 라이소좀, CD20, PIKfyve